Experimental demonstration of 25 GHz wideband chaos in symmetric dual port EDFRL

SHUBHAM MIRG[1], ANKITA JAIN[2], AKASH PANDEY[2], PRADEEP KUMAR K.[1,2,*], AND PASCAL LANDAIS[3]

[1] Department of Electrical Engineering, IIT Kanpur, Kanpur-208016, India
[2] Center for Laser and Photonics, IIT Kanpur, Kanpur-208016, India
[3] School of Electronic Engineering, Dublin City University, Dublin-9, Ireland
[*] Corresponding author: pradeepk@iitk.ac.in

Compiled July 27, 2017

We study dynamics of chaos in dual port erbium-doped fiber ring laser (EDFRL). The laser consists of two erbium-doped fibers, intracavity filters at 1549.30 nm, isolators, and couplers. At both ports, the laser transitions into the chaotic regime for pump currents greater than 100 mA via period doubling route. We calculate the Lyapunov exponents using Rosenstein's algorithm. We obtain positive values for the largest Lyapunov exponent (≈0.2) for embedding dimensions 5, 7, 9 and 11 indicating chaos. We compute the power spectrum of the photocurrents at the output ports of the laser. We observe a bandwidth of ≈ 25 GHz at both ports. This ultra wideband nature of chaos obtained has potential applications in high speed random number generation and communication.

OCIS codes: *(140.1540) Chaos; (140.3560) Lasers, ring; (140.3500) Lasers, erbium.*

http://dx.doi.org/10.1364/ao.XX.XXXXXX

1. INTRODUCTION

Chaotic systems are deterministic but exhibit extreme sensitivity to perturbations in initial conditions [1]. These systems are characterized by a broad bandwidth and rapidly dropping autocorrelation and these exhibit a 'noise-like' long-term behaviour [2]. Thus, the ability of chaos to mask signals makes it suitable for secure communications [3]. Chaotic systems can also be used as sources of physical randomness since at a macroscopic level these systems behave randomly [4]. Chaos based random number generators have been successfully demonstrated [5]. While speed of random number generation and data rates of chaotic communication, using electronic circuits, are limited by chaos bandwidth in the range of few MHz, optical chaos comparatively has a much higher bandwidth and thus have garnered considerable attention for high speed random number generation and secure communication [5–8]. Optical chaos is seen in both semiconductor and fiber laser. Various techniques such as external optical feedback, optical injection, loss modulation exist that can be implemented to obtain chaos in semiconductor lasers [9]. The underlying principle of all the above techniques is to add instability to laser through which chaos is obtained either via period doubling or quasi periodic or intermittent route. Several GHz of chaos bandwidth has been demonstrated with semiconductor lasers [10].

Optical chaos in erbium-doped ring fiber lasers (EDFRL) has been numerically as well as experimentally demonstrated to exhibit rich chaotic behaviour [11–14]. To study chaotic behaviour in EDFRL, the laser is modelled as a three level class B laser owing to its fast decay time of polarization variables [11]. Chaos in EDFRL is obtained by either of the following three techniques or a combination of them: pump modulation [12], loss modulation [15] and loop nonlinearities [11]. Pump and loss modulation generated chaotic waveform bandwidths are limited to MHz range due to relaxation oscillation time of fiber laser. Numerical modelling of EDFRL suggests chaos generation due to nonlinear Kerr effect and chaotic bandwidth to be at least several GHz [11, 13]. Experimental demonstration of the generation of chaos in EDFRL using nonlinear Kerr effect yielded a bandwidth of 2 GHz [14].

In this paper, we demonstrate experimentally large chaotic bandwidth in EDFRL. A near symmetric EDFRL structure with dual port output is employed. As pump currents are increased, well above the threshold, chaotic output is observed at both output ports with similar bandwidth. We employ Rosenstein's algorithm to obtain divergence curves and estimate the largest Laypunov exponent (LLE) [16]. Positive LLE values are obtained at different embedding dimensions indicating presence of chaos. The presence of chaos is further verified by calculating power spectrum, autocorrelation, and phase portraits. Finally, we report a chaos bandwidth of 25 GHz from both ports simultaneously. To the best of our knowledge, this is the largest reported bandwidth of chaos in EDFRL.

The rest of the paper is organized as follows. In section 2

we discuss our experimental setup to generate chaos in EDFRL. In Section 3, we discuss the results of chaos generation in both ports of EDFRL. We describe the various properties of the output signals and indicate the distinction between chaotic and non-chaotic regimes. We conclude by summarizing our work in 4.

2. EXPERIMENTAL SETUP

Fig. 1 shows our experimental setup of the dual port near symmetric erbium-doped fiber ring laser (EDFRL) to generate chaos. The setup is near symmetric with each side consisting of erbium-doped fiber (EDF) of approximately 7 m length, an optical isolator, optical bandpass filter (BPF), and a 3 dB coupler to extract optical signals from the laser. Two 980 nm laser diodes are used to pump the EDFs. Single mode fiber (SMF) patch chords are used to connect optical components of the laser. An optical isolator ensures unidirectional operation of laser. The bandpass filter is has a central wavelength of 1549.30 nm and fixes the lasing wavelength of EDFRL. The two outputs from ports 1 and 2 are converted to photocurrents and measured using a real-time oscilloscope at 50 GSa/s, for pump currents in the range of 70 to 200 mA. The pump currents are adjusted to obtain near equal powers at the two output ports.

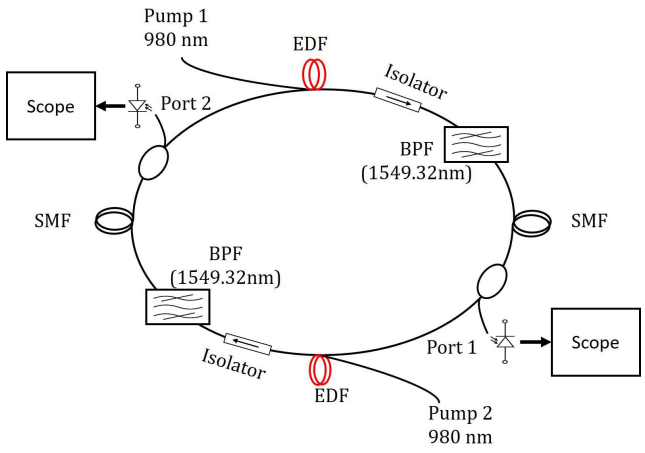

Fig. 1. Experimental setup of dual port near symmetric erbium-doped fiber ring laser to generate chaos. Output from ports 1 and 2 is monitored using real time oscilloscope with sampling rate of 50 GSa/s.

As various electric fields circulate inside the fiber cavity, they are phase modulated due to the nonlinear Kerr effect. Increasing pump current to 100 mA increases the optical power inside cavity and leads to increase in nonlinear phase shift. This modulation provides the perturbation required by the laser for generation of chaos via period doubling route [11].

3. RESULTS AND DISCUSSION

As we increase the pump current, of both EDFs simultaneously, the laser starts lasing at approximately 70 mA. On further increasing the pump currents to about 100 mA, the laser starts bifurcating towards chaotic regime via period doubling. Finally at around 200 mA, the laser is in the chaotic region. The photocurrents at the laser outputs are recorded by the real-time oscilloscope and processed using Rosenstein's algorithm to estimate the LLE [16]. Rosenstein's algorithm works by reconstructing attractor dynamics and calculating the average separation of nearest neighbours as the system evolves. The divergence of trajectories have exponential dependence on Lyapunov exponents of the system, with LLE dominating the growth initially [16]. In the chaotic region with positive LLE, the initial rise in logarithmic plots of divergence curves will be linear with slope determined by LLE. Fig. 2 shows natural logarithm of divergence trajectories at various pump currents and for different embedding dimension (m) of 5, 7, 9, and 11. When pump currents at pumps 1 and 2 are 70 and 72 mA respectively, EDFRL is just at the threshold of lasing. In Figs. 2(a) and (b), we observe that divergence curves do not rise linearly. This is due to the negative Lyapunov exponents at play, indicating absence of chaotic dynamics of the laser at these pump current levels. On further increasing the pump currents to 98 and 94 mA at pumps 1 and 2, the electric fields start interfering due to Kerr effect. In Figs. 2(c) and (d) we see divergence curves are still not linear initially but are much smoother than previous pump currents. This stage is identified as the transition region between chaotic

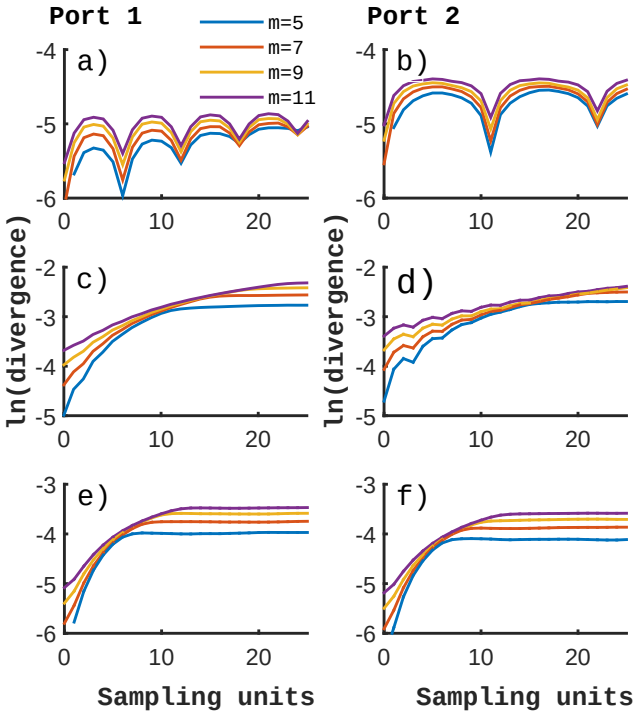

Fig. 2. Natural logarithm of divergence plotted at various embedding dimensions (m). Curves plotted for a), b)- Pump currents 70 and 72 mA c), d)- Pump currents 98 and 94 mA e), f)- Pump currents 200 and 196 mA.

and non-chaotic. However, as we increase the pump currents well above the lasing threshold, 200 and 196 mA for pumps 1 and 2 respectively, the laser transitions into the chaotic regime as seen in Figs. 2(e) and (f). In the chaotic region, we observe an initial linear rise in divergence curves with the slope determined by LLE. However as the system evolves further, other Lyapunov exponents cause the divergence curves to become flat. Table 1 shows the calculated value of LLE exponents for different value of m, all positive and indicative of chaos.

In Fig. 3, we plot the power spectrum of photocurrents obtained at both output ports of the laser. In Fig. 4, we plot the power spectrum on an expanded frequency axis. Discrete spec-

Table 1. Largest Lyapunov exponent (LLE) calculated from the slope of divergence curve for Port 1 from Fig. 2(e) and Port 2 from Fig. 2(f)

Port 1		Port 2	
m	LLE (slope)	m	LLE (slope)
5	0.2313	5	0.2303
7	0.2167	7	0.2172
9	0.1906	9	0.1911
11	0.1658	11	0.1655

tral lines are observed in Figs. 3(a) and (b), for pump currents 70 and 72 mA at pumps 1 and 2. For similar pump currents in Figs. 4(a) and (b), we observe the first peak to be at 90 MHz for both ports and rest of the peaks at the harmonics. The output signals of both ports show periodicity in this region with fundamental frequency of 90 MHz. As the laser goes through the transition region, the power spectrum in Figs. 3(c) and (d), additional frequencies are generated with 15 and 45 MHz fundamental harmonic for ports 1 and 2. This can be observed in Figs. 4(c) and (d).

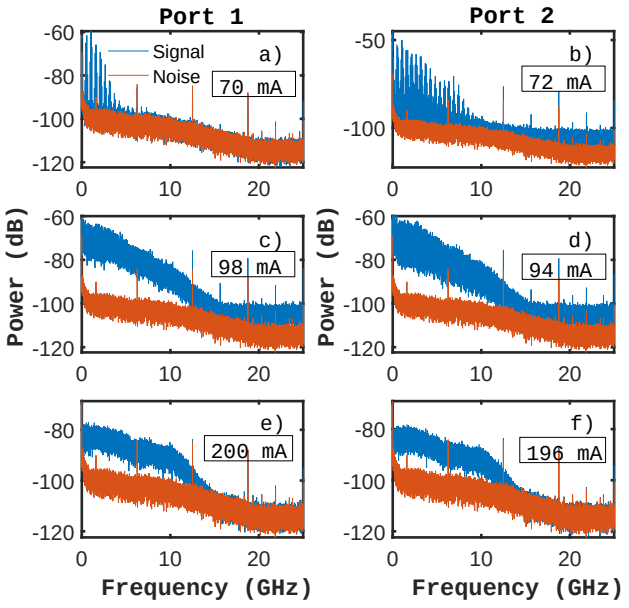

Fig. 3. Power spectrum for output of ports 1 and 2 for different pump currents (blue). For comparison we also plot power spectrum of electronic noise (orange) alone.

This clearly suggests that the laser bifurcation to chaos via the period doubling route. Increasing pump currents further, drives the laser into chaotic region. We plot the power spectrum for this region in Figs. 3(e) and (f), at pump currents of 196 and 200 mA. Due to the laser being chaotic, the discrete spectral lines vanish, as seen in Figs. 4(e) and (f), and a flat power spectrum is obtained with a bandwidth of approximately 25 GHz (two-sided) as shown in Figs. 3(e) and (f). Another set of distinct harmonics peaks with a fundamental frequency of 6.3 GHz are observed in all regions of Fig. 3, irrespective of pump currents. These peaks arise from the amplifier resonances and cannot be

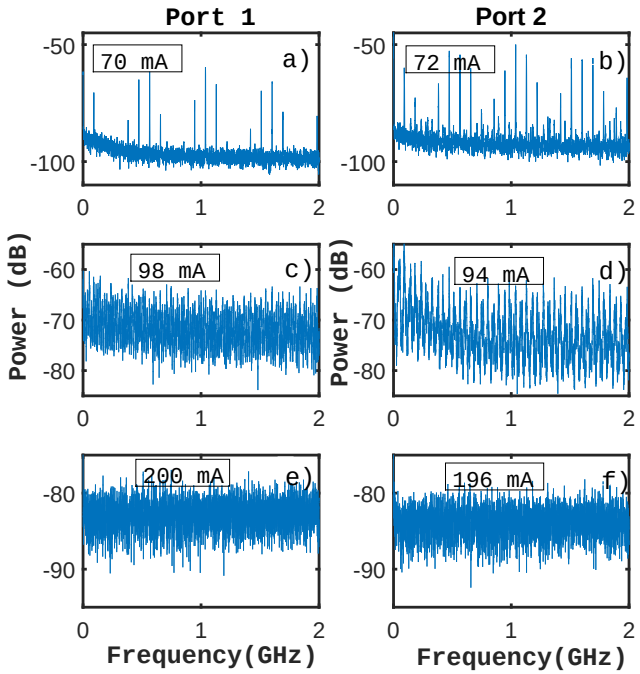

Fig. 4. Power spectrum plot with expanded frequency axis. Signals at both ports show the discrete spectral lines at various pump currents.

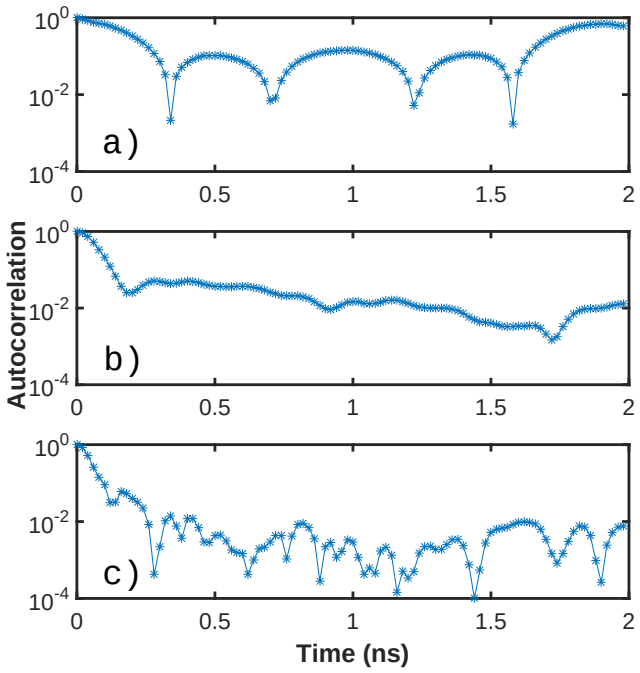

Fig. 5. Autocorrelation of output signal at port 1 for three different regions at different pump currents a) Non-Chaotic, b) Transition, c) Chaotic

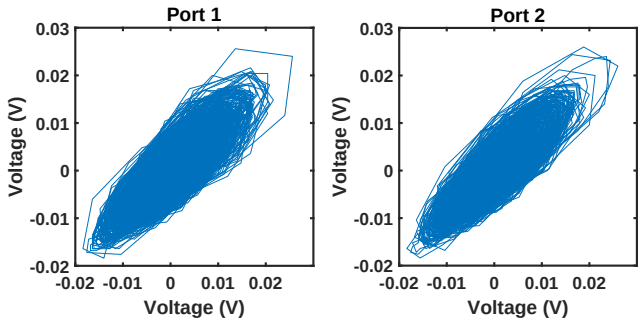

Fig. 6. Phase portrait for ports 1 and 2 and pump currents of 200 and 196 mA at pumps 1 and 2, respectively.

eliminated.

In Fig. 5, we plot autocorrelation of the output signal from port 1. The output signal is correlated with the delayed version of itself and normalized. Autocorrelation is an important parameter for random number generation as it provides an insight to the ability of setup to behave randomly. In the non-chaotic regime, the autocorrelation does not drop significantly as seen in Figs. 5(a) and (b). However, operating the laser in the chaotic region leads to a rapid drop in the value of autocorrelation to almost 10^{-3} in Fig. 5(c). The signal from output port 2 has a similar drop in the value of autocorrelation.

Finally, we plot phase portraits in Fig. 6. Phase portraits represent trajectories of dynamical systems pertaining to different initial conditions in the phase space. We reconstruct the phase portrait using method of delays [16]. A uniform spread in the phase space without any fixed trajectory lines in Fig. 6, is again indicative of chaos.

4. CONCLUSIONS

In summary, we have shown that by using a near symmetric dual port EDFRL setup, ultra high bandwidth chaos can be generated. Increasing pump currents to ≈100 mA, the laser is set on a period doubling route to chaos due to nonlinearities. Chaotic dynamics in the laser are seen at pump currents of ≈200 mA. This is verified by calculating LLE using Rosenstein's algorithm. We obtain positive LLE values of around 0.2 for various embedding dimensions, indicating chaos in the system. Further, when pump currents are increased from threshold, at ≈70 mA, to ≈100 mA, the fundamental frequency in power spectrum reduces by half, hence confirming that the laser takes the period doubling route to chaos. On further increasing pump currents, flat power spectrum with no distinct spectral lines and an almost immediate drop in autocorrelation is observed, due to the onset of chaotic regime. A clear transition from non-chaotic to chaotic region is observed in divergence curves, power spectrum and autocorrelation plots.

The rapid drop in autocorrelation shows the setup is suitable for high speed random number generation. The dual port output further enables us to use the difference method to remove the bias from the random numbers generated [17]. Finally, both ports indicate simultaneous presence of chaos and have similar bandwidths of 25 GHz, the largest seen in EDFRL to best of our knowledge.

5. ACKNOWLEDGEMENT

We acknowledge Marie Curie International Research Staff Exchange Scheme Fellowship, 7th European Community Framework Programme, under Grant 318941 for supporting travel of Pradeep Kumar K. and Ankita Jain.

REFERENCES

1. S. H. Strogatz, *Nonlinear dynamics and chaos: with applications to physics, biology, chemistry, and engineering* (Westview press, 2014).
2. M. P. Kennedy and G. Kolumbán, "Digital communications using chaos," Signal Processing **80**, 1307 – 1320 (2000).
3. G. D. VanWiggeren and R. Roy, "Communication with chaotic lasers," Science **279**, 1198–1200 (1998).
4. T. Stojanovski and L. Kocarev, "Chaos-based random number generators-part i: analysis [cryptography]," IEEE Transactions on Circuits and Systems I: Fundamental Theory and Applications **48**, 281–288 (2001).
5. T. Stojanovski, J. Pihl, and L. Kocarev, "Chaos-based random number generators. part ii: practical realization," IEEE Transactions on Circuits and Systems I: Fundamental Theory and Applications **48**, 382–385 (2001).
6. K. M. Cuomo, A. V. Oppenheim, and S. H. Strogatz, "Synchronization of lorenz-based chaotic circuits with applications to communications," IEEE Transactions on Circuits and Systems II: Analog and Digital Signal Processing **40**, 626–633 (1993).
7. A. Argyris, D. Syvridis, L. Larger, V. Annovazzi-Lodi *et al*., "Chaos-based communications at high bit rates using commercial fibre-optic links," Nature **438**, 343 (2005).
8. K. Ugajin, Y. Terashima, K. Iwakawa, A. Uchida, T. Harayama, K. Yoshimura, and M. Inubushi, "Real-time fast physical random number generator with a photonic integrated circuit," Opt. Express **25**, 6511–6523 (2017).
9. M. Sciamanna and K. A. Shore, "Physics and applications of laser diode chaos," Nature Photonics **9**, 151–162 (2015).
10. K. Hirano, T. Yamazaki, S. Morikatsu, H. Okumura, H. Aida, A. Uchida, S. Yoshimori, K. Yoshimura, T. Harayama, and P. Davis, "Fast random bit generation with bandwidth-enhanced chaos in semiconductor lasers," Opt. Express **18**, 5512–5524 (2010).
11. H. D. I. Abarbanel, M. B. Kennel, M. Buhl, and C. T. Lewis, "Chaotic dynamics in erbium-doped fiber ring lasers," Phys. Rev. A **60**, 2360–2374 (1999).
12. L. Luo, T. J. Tee, and P. L. Chu, "Chaotic behavior in erbium-doped fiber-ring lasers," J. Opt. Soc. Am. B **15**, 972–978 (1998).
13. F. Zhang and P. L. Chu, "Effect of transmission fiber on chaos communication system based on erbium-doped fiber ring laser," Journal of Lightwave Technology **21**, 3334–3343 (2003).
14. L. Zhang, R. Yang, J. M. Qin, and L. Z. Yang, "An experimental study of high frequency chaotic dynamics in an erbium-doped fiber ring laser," Laser Physics **23**, 125104 (2013).
15. S. Z. Ali, M. Islam, and M. Zafrullah, "Comparative analysis of chaotic properties of optical chaos generators," Optik - International Journal for Light and Electron Optics **123**, 950 – 955 (2012).
16. M. T. Rosenstein, J. J. Collins, and C. J. D. Luca, "A practical method for calculating largest lyapunov exponents from small data sets," Physica D: Nonlinear Phenomena **65**, 117 – 134 (1993).
17. I. Reidler, Y. Aviad, M. Rosenbluh, and I. Kanter, "Ultrahigh-speed random number generation based on a chaotic semiconductor laser," Physical review letters **103**, 024102 (2009).